International Journal of Advanced Research and Development
ISSN: 2455-4030
Impact Factor: RJIF 5.24
www.advancedjournal.com
Volume 3; Issue 3; May 2018; Page No. 44-51

Quantum mechanical calculations and spectroscopic investigation (FTIR, FT-Raman and UV-Visible) on (6R, 7R)-7-[(2Z)-2-(2-amino-1, 3-thiazol-4-yl)-2-[(carboxymethoxy) imino] acetamido]-3-ethenyl-8-oxo-5-thia-1-azabicyclo [4.2.0] oct-2-ene-2-carboxylic acid: a Pharmaceutical drug using Density functional theory

P Manjusha[1], Johanan Christian Prasana[2], S Muthu[3*]
[1] Department of Physics, S.D.N.B Vaishnav College for Women, Chromepet Chennai, Tamil Nadu, India
[2] Department of Physics, Madras Christian College, Chennai, Tamil Nadu, India
[3] Department of Physics, Arignar Anna Govt. Arts College, Cheyyar, Tamil Nadu, India

Abstract
Fourier transforms infrared (FT-IR) and FT Raman (FT-RS) and UV-Visible spectra of (6R,7R)-7-[(2Z)-2-(2-amino-1,3-thiazol-4-yl)-2-[(carboxymethoxy)imino]acetamido]-3-ethenyl-8-oxo-5-thia-1-azabicyclo[4.2.0]oct-2-ene-2-carboxylic acid (Cefixime)were recorded and analyzed. Using density functional theory (DFT) calculation (B3LYP) with standard 6-311++G (d,p) basis set the molecular geometry vibrational frequencies, infrared intensities, Raman activity were calculated. The observed FT-IR and FT-Raman data were used to carry out the complete vibrational assignment and analysis of the functional modes of the compound. The thermodynamic functions of Cefixime drug were also performed by B3LYP with basis set 6-311++G(d,p).Potential Energy Distribution (PED) values and the HOMO and LUMO energy gap levels that the energy gap reflects the chemical activity of the molecule and compared with UV Absorption spectra. The Molecular Electrostatic Potential (MEP) mapped onto an isodensity surface has been obtained.

Keywords: FT-IR, FT-Raman, UV-absorption, and DFT

1. Introduction
(6R,7R)-7-[(2Z)-2-(2-amino-1,3-thiazol-4-yl)-2-[(carboxymethoxy)imino]acetamido]-3-ethenyl-8-oxo-5-thia-1-azabicyclo[4.2.0]oct-2-ene-2-carboxylic acid (Cefixime) is a cephalosporin antibiotic. Cefixime is used in the treatment of uncomplicated anogenital gonorrhoea [1]. Cefiximetreats infections of the ear, sinuses, throat, chest and lungs. It is used to treat typhoid fever [2] and the common side effects include diarrhoea, abdominal pain, and nausea. Serious side effects may include allergic reactions and clostridium difficilediarrhoea [3, 4]. It appears to be relatively safe during pregnancy [5]. It works by disrupting the bacteria's cell wall resulting in its death. No major interaction has been observed between cefixime and alcohol [6]. No attempts to theoretically assign the experimental vibrational spectra of (6R,7R)-7-[(2Z)-2-(2-amino-1,3-thiazol-4-yl)-2-[(carboxymethoxy)imino]acetamido]-3-ethenyl-8-oxo-5-thia-1-azabicyclo[4.2.0]oct-2-ene-2-carboxylic acid (Cefixime) have been done yet, to the best of our knowledge.

2. Experimental detail
The Cefixime drug was purchased from Unichem laboratory with stated purity 99 % and was used as such without further purification to record FT-IR and FT - Raman spectra. The molecular structure of Cefixime is shown in Fig.1. The FT-IR spectra of Cefiximeis recorded in evacuation mode on Bruker IFS 66V spectrophotometer in the region 4000 – 450 cm^{-1} using KBr pellet technique (solid phase) with 4.0 cm^{-1} resolutions, The FT Raman spectrum is recorded using 1064nm line of Nd: YAG laser on Bruker IFS 66V spectrophotometer equipped with FRA 106 FT Raman module accessory as excitation wavelength in the region 4000 –50 cm^{-1}. The spectral measurements were carried out at Sophisticated Analysis Instrumentation Facility (SAIF), Indian Institute of Technology (IIT), Chennai, India. The UV–vis spectrum of the molecule was also recorded by the UV–Visible spectrophotometer in the wavelength region 200–500 nm using DMSO as a solvent.

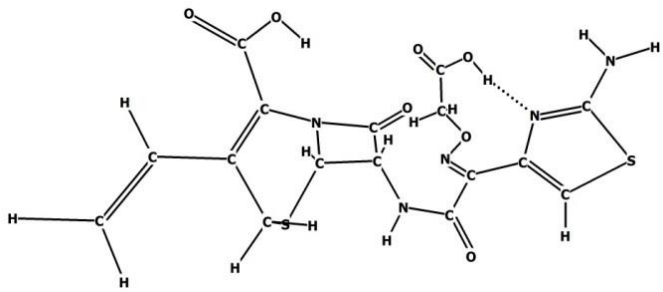

Fig 1: Molecular structure of Cefixime

3. Computational Detail
The entire calculations conducted for the present work were performed at B3LYP levels included in the Gaussian 09W package [6] program together with 6-311++ G(d,p) basis set function of the density functional theory (DFT) utilizing

gradient geometry optimization [7]. Initial geometry was minimized without any constraint in the potential energy surface adopting the standard 6-311++ G (d, p) basis set generated from standard geometrical parameters. This geometry was reoptimized again at B3LYP level, using basis set 6-311++ G(d,p) for better description. The optimized structural parameters were used at DFT levels in the vibrational frequency calculations to characterize all stationary points as minima. At the optimized structure of the examined species, no imaginary frequency modes were obtained proving that a true minimum on the potential energy surface was found. We have utilized the gradient corrected density functional theory [8] with the three parameter hybrid functional (B3) [9] for the exchange part and the Lee-Yang – Parr (LYP) correlation function [10], accepted as a cost effective approach for the computation of molecular structure, vibrational frequencies and energies of optimized structures. The symmetry considerations, vibrational frequency assignments were made with a high degree of accuracy by combining the results using Gauss view program [11]. The Thermodynamic properties by way of statistical mechanics were provided by the finally calculated normal mode vibrational frequencies. Zero point vibrational energy was calculated and there is a standard scaling factor introduced to compensate for the errors arising from the basis set incompleteness and to neglect of vibrational an harmonicity.

4. Results and Discussions

4.1 Geometrical Structure

The optimized structure parameters of (6R,7R)-7-[(2Z)-2-(2-amino-1,3-thiazol-4-yl)-2-[(carboxymethoxy)imino]acetamido]-3-ethenyl-8-oxo-5-thia-1-azabicyclo[4.2.0]oct-2-ene-2-carboxylic acid calculated by DFT-B3LYP levels with the 6-311++G(d,p) basis set. The labelling of atoms in Cefixime is given in Fig.2. Comparison table for the calculated bond lengths and angles for Cefixime with those of experimentally available x-ray diffraction data [12] are listed in the Table1. Optimized bond angles were slightly larger than the experimental values, due to the reason theoretical calculations belong to isolated molecules in gaseous phase and the experimental results belong to molecules in solid phase. Comparing bond angles and lengths of B3LYP the formers are on higher side than the latter and the calculated values correlates well compared with the experimental results. In spite of the differences calculated geometric parameters represent a good approximation and they are the value the bases for calculating vibration frequencies and thermodynamical properties.

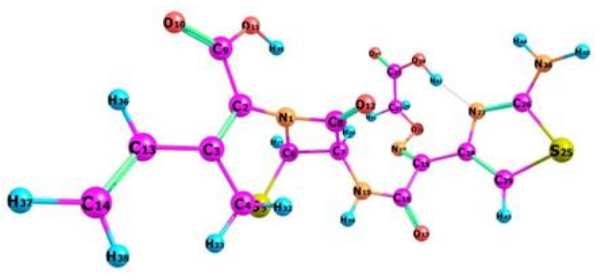

Fig 2: Optimized geometric structure with atoms numbering of cefixime

Table 1: Geometrical parameters optimized in Cefiximebond length(Å) and bond angle(°) with 6-311++G (d,p) basis set

Bond Angle(°)	B3LYP/6-31++G(d,p)	Experimental value*
C_2-N_1-C_6	113.6	113.9
C_2-N_1-C_7	125.2	125.7
N_1-C_2-C_3	122.5	122.7
N_1-C_2-N_{15}	115.4	115.8
C_6-N_1-C_7	121.2	121.6
N_1-C_6-S_5	122.5	122.6
N_1-C_6-C_8	119	119.6
C_3-C_2-N_{15}	122	122.5
C_2-C_3-C_4	121.6	121.8
C_2-C_3-C_{16}	119.5	119.9
C_4-C_3-C_{16}	118.9	119.3
C_3-C_4-S_5	116.7	117.4
S_5-C_4-C_{14}	122	122.5
C_4-S_5-C_6	123	123.4
C_4-S_5-O_{17}	122.1	122.4
C_4-C_{14}-O_{23}	111.4	111.7
C_4-C_{14}-O_{24}	111.4	111.6
C_4-C_{14}-S_{25}	111.3	111.8
C_6-S_5-O_{17}	114.9	115.4
S_5-C_6-C_8	118.5	118.7
C_6-C_8-C_9	119.4	119.7
C_6-C_8-C_{13}	120.2	120.8
C_9-C_8-C_{13}	120.4	120.7
C_8-C_9-O_{10}	119.8	120.4
C_8-C_9-C_{18}	119.7	120.2
C_8-C_{13}-O_{12}	119.5	120.0
C_8-C_{13}-C_{22}	119.8	120.1
O_{10}-C_9-C_{18}	120.4	120.7
C_9-O_{10}-O_{11}	120.1	122.7
C_9-O_{10}-N_{19}	119.7	120.4
O_{11}-O_{10}-N_{19}	120.3	120.6
O_{10}-O_{11}-O_{12}	119.8	120.4
O_{10}-O_{11}-O_{20}	120.1	120.5
O_{12}-O_{11}-O_{20}	120.1	120.6
O_{11}-O_{12}-C_{13}	120.5	120.9
O_{11}-O_{12}-C_{21}	120.1	120.7
C_{13}-O_{12}-C_{21}	119.5	119.9
O_{12}-C_{13}-C_{22}	120.7	121.4
O_{23}-C_{14}-O_{24}	107.7	107.9
O_{23}-C_{14}-S_{25}	107.7	107.9
O_{24}-C_{14}-S_{25}	107.2	107.6

Ref taken from [12]

4.2 Thermodynamic Properties

On the basis of vibrational analysis, the statically thermodynamic functions: heat capacity (C^0m), entropy (S^0m), and enthalpy changes (ΔH^0m) for the title molecule are obtained from the theoretical frequencies and listed in Table 2. From Table 2, all the values of C^0m, S^0m and H^0m are increasing with temperature ranging from100K to 1000K due to the fact that the molecular vibrational intensities increase with temperature. The correlation equations between heat capacity, entropy, enthalpy and temperatures are fitted by quadratic formulas and the corresponding fitting factors (R^2) for these thermodynamic properties are 0.99936, 0.99986 and 0.99917respectively. The corresponding fitting equations are as follows and the correlation graphs of those shown in Fig.3.

C^0p, m =57.87129+1.52125T-7.03343x$10^{-4}T^2$ (R^2=0.99936)

S^0m =319.4752+1.83006T-5.12389x$10^{-4}T^2$ (R^2=0.99986)

H^0m = -23.26313+0.24487T+3.67594 x$10^{-4}T^2$(R^2=0.99917)
All these thermodynamic data provide helpful information for the further study on the (6R,7R)-7-[(2Z)-2-(2-amino-1,3-thiazol-4-yl)-2-[(carboxymethoxy)imino]acetamido]-3-ethenyl-8-oxo-5-thia-1-azabicyclo[4.2.0]oct-2-ene-2-carboxylic acid. They can be used to compute the other thermodynamic parameters according to relationships of thermodynamic functions and to estimate the directions of chemical reactions according to the second law of thermodynamics in thermo chemical field [13].

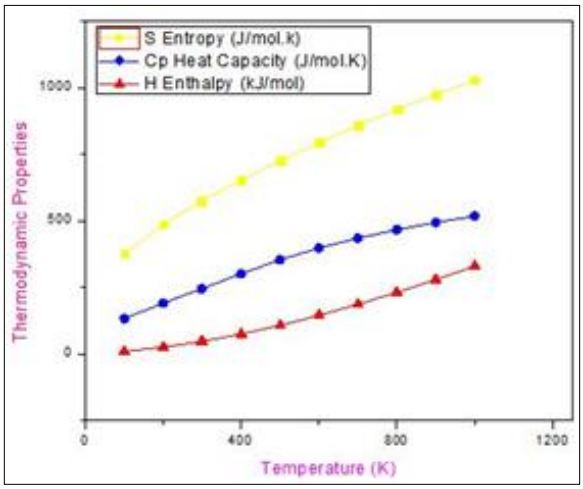

Fig 3: Correlation plot of thermodynamic properties at different temperature of cefixime

Table 2: Temperature dependence of thermodynamic properties of Cefixime at B3LYP/6-311++G (d,p)

T (K)	S (J/mol.K)	Cp (J/mol.K)	ddH (kJ/mol)
100.00	489.944	200.968	12.630
200.00	668.846	329.649	39.177
298.15	823.312	450.421	77.542
300.00	826.105	452.583	78.378
400.00	971.508	560.272	129.179
500.00	1106.327	648.041	189.760
600.00	1230.870	717.527	258.175
700.00	1345.777	772.665	335.788
800.00	1451.955	817.102	412.353
900.00	1550.367	853.541	495.943
1000.00	1641.914	883.866	582.858

4.3 Vibrational Assignments

The title compound consists of 45 atoms, which has 129 normal modes of vibration. Modes of title molecule have been assigned according to the detailed vibrations of the individual atoms. All the 129 fundamental vibrations are active in both IR absorption and Raman scattering. Fig.4 and Fig.5 represents the experimental and theoretical FT-IR and FT-Raman spectra of the molecule respectively. The experimental FT-IR and FT-Raman together with the calculated wave numbers are tabulated in Table 3.On the consideration of basis of a group vibrational concept and calculated vibrational wave numbers the fundamental modes of the title compound were assigned. Chem craft, which is a graphical interface, was used to assign the calculated wave number on the experimental results. It should be noted that Gaussian 09 package does not calculate the Raman intensities. The Raman activities were transformed into Raman intensities using Raint program [14] by the experimental

$I_i = 10^{-12}(\upsilon - \upsilon_\circ)^4(1/\upsilon_i)$ s where,

I_i is the Raman intensity.,

s is the Raman scattering activities.,

υ_i is the wave number of normal modes and

$\upsilon_\circ$ denotes the wave number of the excitation laser [15]

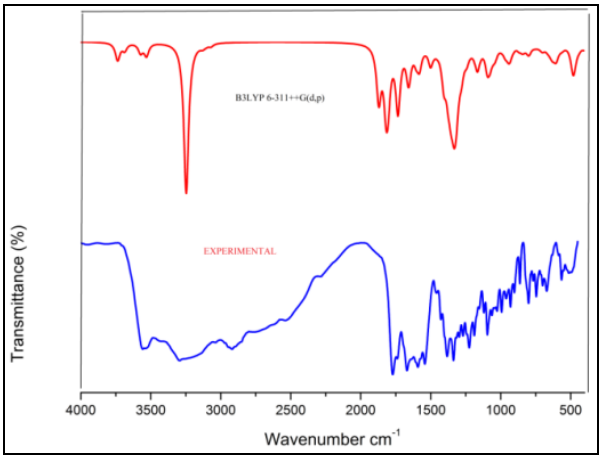

Fig 4: FT-IR spectra of Cefixime (Experimental, B3LYP/6-311++G (d,p)

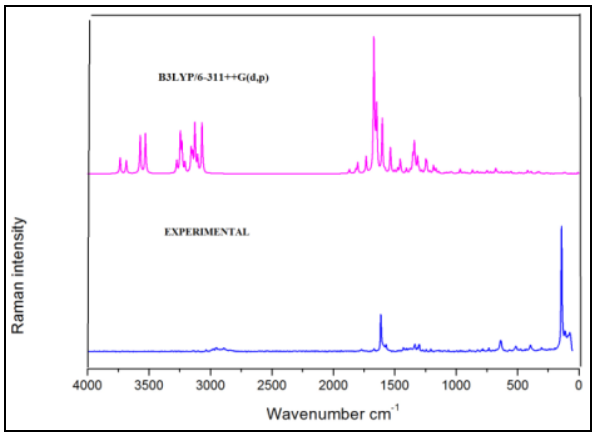

Fig 5: FT-Raman Spectra of Cefixime (Experimental, B3LYP/6-311++G (d,p)

Table 3: Observed and calculated vibrational frequencies of Cefiximeat B3LYP method with 6-311++G(d,p)basisset

Mode no.	Frequencies		Calculated (cm^{-1})		IR Intensity	Raman Activity	Vibrational assignments (>10%ped)
	Unscaled	Scaled	FT-IR	FT-Raman			
1	3735	3672	-	3754vw	139.454	69.71	γOH(100)
2	3685	3622	-	-	56.655	57.20	γNH(100)
3	3572	3511	3557vw	3554vw	75.010	164.71	γNH(100)
4	3529	3469	3539vw	-	99.196	173.77	γNH(100)
5	3275	3219	3292s	-	14.305	52.41	γCH(99)
6	3245	3190	-	-	1181.912	170.80	γOH(99)
7	3232	3177	-	-	5.035	119.81	γCH(100)
8	3208	3153	-	-	14.107	44.82	γCH(92)
9	3158	3104	-	3162vw	3.016	99.60	γCH(78)
10	3147	3093	-	-	2.287	72.66	γCH(98)
11	3128	3074	-	-	22.051	172.39	γCH(97)
12	3124	3071	-	3121vw	3.036	59.09	γCH(99)
13	3105	3052	-	-	9.328	67.10	γCH(97)
14	3069	3017	-	-	18.674	176.60	γCH(100)
15	3067	3015	3036w	3051w	2.895	51.49	γCH(92)
16	1732	1703	1738w	1751vw	503.405	71.43	γOC(80)
17	1669	1599	1661s	1684vw	5.273	574.69	γCC(55)+βHCH(18)
18	1657	1587	-	1667m	259.328	62.58	γNC(12)+βHNH(60)
19	1646	1577	-	-	24.773	272.81	γNC(70)
20	1602	1534	1591s	1612vs	86.493	234.58	γCC(65)
21	1579	1513	-	1570m	153.765	11.35	γNC(72)+ βHNH(19)
22	1535	1470	1541vs	-	3.445	112.64	γNC(70)
23	1500	1437	-	1515vw	136.532	11.99	βHNC(49)+βHCN(16)
24	1475	1413	-	1482vw	11.776	21.66	βHCH(62)+τHCSC(28)
25	1455	1394	1457w	1459vw	8.281	57.62	βHCC(12)+βHCH(62)
26	1448	1387	1426m	1428w	9.806	7.12	βHCH(85)
27	1404	1345	-	1405w	248.414	21.71	γNC(26)+γCC(23)
28	1374	1317	1382vs	1382vw	218.376	13.74	βHOC(30)
29	1358	1301	-	1359vw	71.718	2.88	τHCON(71)
30	1353	1296	-	-	232.798	71.43	βHOC(16)
31	1340	1284	-	-	61.785	124.68	γCC(15)+βHCC(56)
32	1336	1280	1337vs	1336vw	39.306	5.98	βHNC(17)+βHCN(52)
33	1330	1274	-	-	326.255	13.84	γOC(13)+βHOC(23)
34	1316	1261	-	1318vw	158.725	16.88	βHOC(14)+βHCS(10)
35	1314	1259	1317vw	-	142.661	54.65	γNC(20)+γ(17)+βHNC(12)
36	1302	1247	1296m	1300s	50.493	14.40	βHOC(11)+βHCS(48)
37	1281	1227	-	-	9.535	3.90	βHCO(66)+τHCON(16)
38	1279	1225	1269s	1276vw	149.940	7.25	γNC(14)+γNC(10)+τHCSC(29)
39	1247	1195	-	-	21.370	51.64	βHCS(12)+ τHCSC(19)+ τHCSC(15)
40	1240	1188	-	1241w	50.921	17.19	γOC(27)+βHOC(24)
41	1238	1186	1224vs	-	13.755	24.49	τHCSC(18)+τHCCN(12)
42	1213	1162	-	1206W	8.865	8.70	γNC(36)
43	1187	1137	1188s	-	5.069	5.80	τHCCN(50)
44	1184	1134	-	1180vw	19.121	30.16	βHCS(30)+τHCSC(19)
45	1166	1117	-	-	27.799	6.80	γOC(24)+βHOC(18)+ τHCSC(12)
46	1164	1115	1153m	-	134.975	14.97	γCC(13)+βHCS(32)
47	1142	1094	1120s	1127vw	14.739	8.75	βHNC(27)+βHCS(32)
48	1093	1047	1094vs	-	168.468	2.90	γOC(50)
49	1074	1029	1062m	1077vw	99.823	5.09	γOC(17)+γNC(12)+ βHCC(18)
50	1055	1010	-	1064vw	29.098	1.93	γNC(32)+ τHCCC(21)
51	1050	1006	-	1051w	2.941	4.35	γNC(11)+ τHCCC(50)
52	1039	995	-	-	57.623	5.22	γOC(13)+γON(18)+τHCON(12)+optOCOC(16)
53	1034	991	-	-	9.249	1.59	βHCC(27)
54	1030	987	1026m	1029vw	6.871	1.77	γNC(14)+βHCC(15)
55	992	950	993vs	994vw	13.370	2.39	γOC(10)+γCC(36)
56	968	927	963vs	-	12.775	11.30	γNC(26)
57	965	925	960s	963vw	46.811	8.59	τHCCC(96)
58	944	905	-	956vw	45.515	0.78	τHOCC(66)
59	941	901	-	-	23.143	2.46	βCCN(18)+τHOCC(13)
60	931	892	929vs	-	65.443	5.14	γON(43)+τHOCC(10)

61	909	871	902s	912vw	13.928	3.29	γCC(13)+βCNC(24)
62	867	831	-	-	29.658	8.06	γOC(26)+γCC(33)+βOCO(12)
63	866	830	862vs	863vw	1.684	7.77	βHCS(11)+τHCSC(11)+τCCCN(10)
64	842	807	-	-	43.000	2.56	γSC(62)
65	827	793	-	825w	11.233	10.21	γNC(17)
66	804	770	800vs	815vw	19.758	4.55	optONCC(17)
67	796	763	-	795vw	56.057	2.58	τHCSC(10)+optONCC(16)
68	782	749	-	782m	5.254	4.13	βCCN(12)+optOCOC(22)
69	758	726	768s	-	10.183	2.01	τHCSC(69)+optONCC(19)
70	748	717	74vs	742vw	4.826	12.69	τCCCN(10)+optOCOC(24)optCCCC(10)+
71	737	706	-	734m	6.378	1.66	γCC(12)+βOCO(26)
72	720	690	-	721vw	10.330	7.72	βCCN(14)optNCCC(14)
73	700	671	700s	702vw	41.632	3.92	βNCC(10)+τHNCC(12)+optCCNC(11)
74	679	651	-	679vw	5.100	14.85	βOCO(12)+τHCCC(14)
75	675	646	671vs	-	1.384	11.89	βSCC(16)+βCCN(17)
76	666	638	-	-	7.545	1.66	γSC(18)
77	659	632	-	-	20.988	4.29	βSCC(10)+βOCO(21)+βOCC(13)
78	644	617	-	638vs	26.152	3.13	τHNCC(20)+optNSNC(11)+optCCNC(11)
79	629	603	-	-	66.271	8.36	τHNCC(19)
80	610	584	-	-	40.328	1.19	βCCC(10)+βCCN(16)
81	601	576	-	602vw	51.517	0.47	τHNCC(25)+optNSNC(22)
82	600	574	-	-	23.452	4.06	τHOCC(61)
83	584	559	585w	-	5.525	7.05	βSCC(25)+βCNC(12)
84	577	553	-	-	6.610	0.93	βOCO(13)+optNSNC(11)+optCCNC(13)
85	563	539	564s	567w	16.881	3.38	optOCOC(29)
86	552	529	529vw	-	11.113	9.03	optOCOC(25)
87	527	505	512w	-	3.083	2.35	-
88	499	478	496vw	514s	3.731	0.35	-
89	489	468	-	-	18.725	4.37	τCCNC(14)
90	481	461	-	-	179.516	0.43	τHNCS(71)
91	468	448	-	473w	66.503	3.42	γCC(11)+βOCO(11)
92	439	421	-	434vw	24.052	2.38	βOCN(10)+τONCC(14)
93	418	400	-	-	3.009	13.89	βCCC(17)
94	402	385	-	-	18.332	2.60	βOCC(17)
95	394	378	-	395s	2.246	1.80	βCNC(11)+βNCN(37)
96	388	372	-	-	21.284	7.96	βOCC(11)
97	348	333	-	-	7.257	2.00	βOCC(10)+optCCCC(10)
98	335	321	-	335vw	6.519	6.16	βCON(12)
99	327	314	-	-	6.661	2.13	βCCO(10)
100	323	309	-	-	0.070	5.27	βSCN(19)+βCCC(13)
101	313	300	-	-	11.780	0.62	βOCC(12)+βCCO(10)+τHNCS(34)
102	307	294	-	304m	40.444	0.60	βOCC(14)+βCCO(10)+τHNCS(49)
103	267	256	-	279Vvw	8.304	1.57	τSCCC(49)+optNSNC(13)
104	262	251	-	-	2.190	1.20	βNCC(37)+optOCNC(11)
105	255	244	-	255vw	8.396	0.96	βCCC(13)+τCNCC(10)
106	246	236	-	244vw	8.141	1.62	βCCC(53)
107	221	211	-	223vw	0.215	0.50	βCNCC(12)+τONCC(20)
108	192	184	-	191w	2.677	1.45	βCCC(40)
109	183	175	-	-	6.089	1.12	βNCC(10)+τCONC(20)+τONCC(13)
110	162	155	-	-	4.558	0.42	βNCC(12)+optSCNC(14)+optNCCC(10)
111	156	149	-	142vs	0.277	1.33	βNCC(12)
112	124	119	-	-	3.997	2.14	optCNCC(31)+optSCNC(12)
113	116	111	-	113s	0.318	2.61	βCCC(13)+τCNCC(11)
114	110	106	-		1.663	2.27	τCCCC(12)+τCCCN(12)+τCCNC(14)
115	95	91	-		0.526	1.00	τOCCO(33)+τCONC(15)
116	85	81	-	84vw	0.918	1.90	τOCCO(16)+τCONC(16)
117	75	72	-	75s	0.467	0.61	τCCCC(26)
118	74	71	-	-	0.238	2.45	βCCN(11)+τCCCC(12)+optNCCC(16)
119	71	68	-	-	1.359	2.24	τOCCN(78)
120	53	51	-	-	0.612	2.26	τCCCC(18)
121	49	47	-	-	0.166	2.20	τNCCC(57)
122	43	41	-	-	5.401	3.56	τCCNC(10)+τCCCN(19)+optCCCN(11)
123	34	33	-	-	5.289	0.48	τCCNC(11)+τCCON(19)+τONCC(18)

124	20	19	-	-	1.446	2.28	τCCNC(13)+τCCON(19)+τONCC(14)
125	16	15	-	-	0.924	2.39	τCNCC(13)+τCCCN(42)+τCCNC(11)
126	9	8	-	-	1.33	4.55	τCNCC(68)+τCCCN(10)
ϒ-stretching,β-bending,τ-torsion,Opt-out of the plane							

4.3.1 C-H Stretching Modes

The hetero aromatic structure shows the presence of C-H stretching vibrations in the region 3300 cm^{-1} - 3000 cm^{-1}which is characteristic region for the ready identification of C-H stretching vibrations. In hetero cyclic compound C-H vibration absorption bands are usually weak; in many cases it is too weak for detection. In this region, the bands are not affected, appreciably by the nature of the substituent Gunasekaran *et al*. [16] identified the presence of C-H stretching vibrations in the region 2990-2820 $cm^{-1.}$ The bands observed at 3292, 3036 cm^{-1} in FT-IR and bands at 3162, 3121, 3051 cm^{-1} in FT-Raman are assigned to C-H stretching. For the same C-H vibration the B3LYP/6-311++(d, p) gives the frequency values in the range 3275,3158,3124,3067 cm^{-1} respectively. In general, the aromatic C-H stretching vibrations calculated theoretically are in good agreement with the experimentally reported values [17-19] in the region 3300-3000 cm^{-1}.

4.3.2 C-C Vibrations

The C-C aromatic stretching vibrations gives rise to characteristic bands in both the observed IR and Raman spectra, covering the spectral range from 1600 – 1400 cm^{-1}. In general, the bands are of variable intensity and according to Varsanyi [20] the five bands in this region are observed at 1625-1590,1590-1575,1540-1470,1465-1430 and 1380-1280 cm^{-1}. The FT-IR and FT-Raman values obtained from C-C stretching are 1661, 1591 and 1684, 1612 cm^{-1} respectively. The calculated frequency values obtained from B3LYP level are 1669, 1602 $cm^{-1.}$These frequencies have been assigned to C-C stretching vibrations. The predicted frequency of B3LYP agrees well with the observed ones.

4.3.3 N-H Vibrations

The vibrations belonging to N–H stretching always occur in region 3450-3250cm^{-1}. In this study, the FT-IR N-H stretching band is observed experimentally at 3557 and 3539 cm^{-1} and for FT RAMAN at 3554cm^{-1}. The theoretically calculated values by B3LYP/6-311++G(d,p) method at 3572 and 3529 cm^{-1} is assigned to N-H stretching vibrations. The PED contribution of these modes is 100%.

4.4 Homo – LumoAnalysis

Many organic molecules, constituting conjugated π electrons characterized by large values of molecular first hyperpolarizability were analyzed by means of vibrational spectroscopy [21, 22]. In most cases, even in the absence of inversion symmetry, the strongest bands in the Raman spectrum are weak in the IR spectrum and vice versa. But the intramolecular charge-transfer from the donor to accepter group through a single-double bond conjugated path, polarizability making IR and Raman activity strong at the same time. It is also observed in title molecule that the bands in FTIR spectrum have their counterparts in Raman showing that the relative intensities in IR and Raman spectra are comparable resulting from the electron cloud movement through πconjugated frame work from electron donor to electron acceptor groups. The analysis of the wave function indicates that the electron absorption corresponds to the transition from the ground to the first excited state and is mainly described by one-electron excitation from the highest occupied molecular orbital (HOMO) to the lowest unoccupied molecular orbital (LUMO). The Highest Occupied Molecular orbitals (HOMOs) and Lowest unoccupied Molecular orbitals (LUMOs) are named as Frontier molecular orbital's(FMOs).The HOMO is located over phenyl ring; the HOMO → LUMO transition implies an electron density transfer to carboxylic acid group from phenyl ring. Moreover, these orbitals significantly overlap in title molecule.

The HOMO–LUMO energy gap (6R,7R)-7-[(2Z)-2-(2-amino-1,3-thiazol-4-yl)-2-[(carboxymethoxy)imino]acetamido]-3-ethenyl-8-oxo-5-thia-1-azabicyclo[4.2.0]oct-2-ene-2-carboxylic acid calculated at B3LYP/6-311++(d, p) level is sketched in Fig. 6. It reveals that the energy gap reflect the chemical activity of the molecule. HOMO is the ability to donate an electron: HOMO energy = - 6.7343 eVLUMO energy= -2.866 eVHOMO-LUMO energy gap = 3.8675 eVAlso the relatively lower HOMO and LUMO energy gap explains the eventual charge-transfer interactions taking place within the molecule.

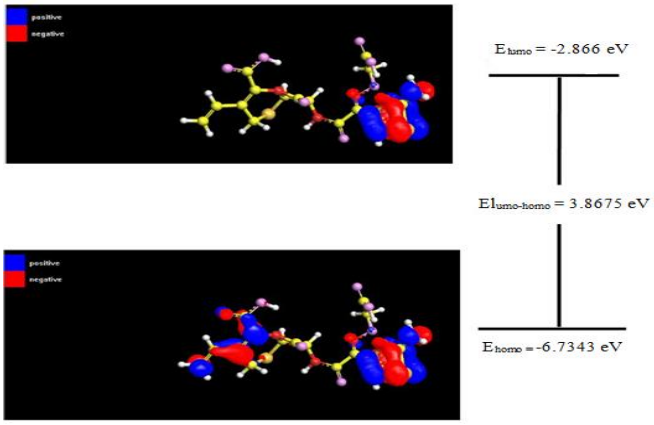

Fig 6: Highest and lowest occupied molecular orbitals of Cefixime obtained by B3LYP/6-311++G(d,p) method.

4.5 UV-visible spectral analysis

The experimental UV-Visible spectrum of Cefixime is shown in Fig. 7. The theoretical excitation energies, absorption wavelength and oscillator strength were calculated by TD-DFT method with 6-311++G(d,p) basis set. All the calculations were performed assuming the title compound was in liquid phase with DMSO as solvent. The experimental and calculated results of UV-Visible spectral data were listed in Table 6. Experimentally measured λ_{max} values 348,332,323 nm showed a good agreement with the theoretical wavelengths 400.55,351.35,335.02 nm. The UV-Visible spectral analysis indicates that the electron absorption

corresponds to the transition from the ground sate to the first excited state [23, 24]. It is mainly described by an electron excitation from highest occupied molecular orbital (HOMO) to the lowest occupied molecular orbital (LUMO). The band gap energy was calculated using the formula E = hc/λ, here "h" and "c'' are constants; λ is the cut-off wavelength. Energy gap of title molecule is calculated experimentally by UV-Visible spectrum is 3.841eV, Energy gap is calculated theoretically by TD-DFT method is 3.703 eV and from HOMO-LUMO diagram is 3.8675 eV.

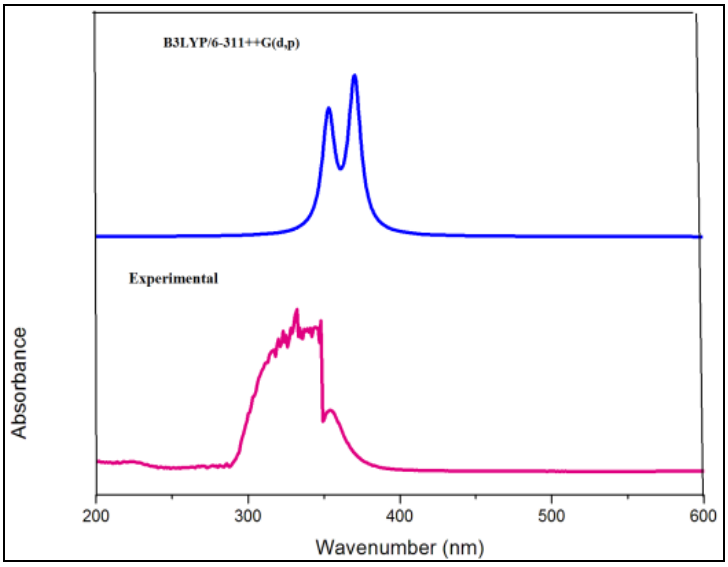

Fig 7: UV-Vis Spectra of Cefixime (Experimental, B3LYP/6-311++G (d,p)

Table 4: Calculated energy values of Cefixime byB3LYP/6-311++G (d,p) method

Basis set	B3LYP/6- 11++G (d,p)
E_{HOMO}	-6.7343
E_{LUMO}	-2.866
Ionization potential	6.7343
Electron affinity	2.866
Electro negativity	-4.80015
Chemical potential	4.80015
Chemical hardness	-1.93415
Chemical softness	0.258511
Electrophilicity index	-5.95647
Energy gap	3.8675

Table 5: UV-vis band gap energy E (eV) and oscillator strength (f) of Cefixime

Experimental		Theoretical				Assignments
Max (nm)	Band gap(eV)	Max (nm)	Band gap(eV)	Energy (cm^{-1})	f	
348	3.565	400.55	3.101	24965	0.0002	H-2->LUMO (71%),H-2->L+1 (13%)H-4->LUMO(5%), H-3->LUMO (3%)
332	3.737	351.35	3.534	28461	0.1079	H-4->L+1 (10%), H-1->LUMO (15%), H-1->L+1 (57%)H-4->LUMO (2%), H-2->L+1 (3%), HOMO->L+1 (7%)
323	3.841	335.02	3.703	29848	0.1408	HOMO>LUMO(80%),HOMO->L+1 (14%)H-1->LUMO (3%)

5. Conclusion

The FT-IR and FT-Raman have been recorded and the detailed vibrational assignment is presented for the title compound, (6R,7R)-7-[(2Z)-2-(2-amino-1,3-thiazol-4-yl)-2-[(carboxymethoxy)imino]acetamido]-3-ethenyl-8-oxo-5-thia-1-azabicyclo[4.2.0]oct-2-ene-2-carboxylic acid for the first time. The equilibrium geometries and vibrational frequencies of the title compound have been calculated at B3LYP levels using 6-311++G (d, p) basis set. The difference between the corresponding wave numbers (observed and calculated) is very small for most of the fundamentals. The same trend is also reflected in the optimized parameters. Therefore, the results presented in this work for the title compound indicate that this level of theory is reliable for prediction of both the infrared and Raman spectra of the large organic molecules. The calculated HOMO and LUMO energy gap is confirmed the presence of charge-transfer within the molecule. The electric dipole moments and the first order hyperpolarizabilities of the compound have been calculated by B3LYP method with 6-311++G (d, p) basis set. Furthermore, the thermodynamic parameters and properties of the compound have been calculated. It was seen that the heat

capacities, entropies and enthalpies increasing temperature owing to the intensities of the molecular vibrations increase with increasing temperature.

6. References

1. WHO Model List of Essential Medicines (19th List) (PDF). World Health Organization. April 2015. Archived (PDF) from the original on 13 December 2016. Retrieved 8 December 2016.
2. Mechanism of Therapeutic Effectiveness of Cefixime against Typhoid Fever". Antimicrobial Agents and Chemotherapy. September 2001. Archived from the original on. 2015. Retrieved 7 April 2016
3. Cefixime. The American Society of Health—System Pharmacists. Archived from the original on 27 November 2016.Retrieved 8 December 2016.
4. WHO Model Formulary 2008 (PDF).World Health Organization. 2009, p. 107. ISBN 9789241547659. Archived (PDF) from the original on 13 December 2016. Retrieved 8 December 2016.
5. Cefixime (Suprax) Use During Pregnancy. Archived from the original on. 2016, 12-20.
6. Choices NHS. Medicines information links. www.nhs.uk. NHS Choices. Archived from the original on. 2015. Retrieved 22 August 2016.
7. Schlegel HB, Comput J. Chem. 1982; 3:214.
8. Hohenberg P, Kohn W. Phys. Rev. B. 1964; 864:136.
9. Becke AD, J Chem. Phys. 1993; 98:5648.
10. Lee C, Yang W, Parr RG. Phys Rev. 1988; B37:785.
11. Frisch A, Neilson AB, Holder AJ. Gauss view user manual, Gaussian Inc., Pittsburgh, P.A, 2000.
12. Casini A, DeSimone G, Pedone C, Antel J, Scozzafava A, Supuran CT. Acta Cryst. 2005; A61:c242.
13. Bopp F, Meixner J, Kestin J. Thermodynamics and Statistical Mechanics, Fifth Ed., Acadamic Press Inc., Ltd., London, New York, 1967.
14. Michalska D, Raint Program. Wroclam University of Technology, 2003.
15. Michalska D, Wysokinski R. Chem. Phys. Lett. 2005; 403:211.
16. Gunasekaran S, Usha Desai. Asian Journal of Physics. 2000; 9:382.
17. Colthup NB, Daly LH, Wiberly SE. Introduction to Infrared and Raman Spectroscopy, Academic Press, New York. 1964; 74:221-226.
18. Gunasekaran S, Seshadri S, Muthu S, Kumaresan S, Arun Balaji R. Spectrochimica Acta part A. 2000; 70:550-556.
19. WilsonJr EB, Decius DC, Cross PC. Molecular vibrations, McGraw Hill, New York, 1995.
20. Varasanyi G. Vibrational spectra of Benzene derivatives (Academics press, New York), 1969.
21. Vijayakumar T, Hubertjee I, Nair CPR, Jayakumar VS. J Chem. Phys. 2008; 343:83-99.
22. Palafox MA. Int. J. Quant. Chem. 2000; 77:661-684.
23. Subramanian Sundarganesan N, Jayabharathi N. J Molecular structure, spectroscopic (FT-IR, FT-Raman, NMR, UV) studies and first-order molecular hyperpolarizabilities of 1,2-bis(3-methoxy-4-hydroxybenzylidene) hydrazine by density functional method, Spectrochim. Acta. 2010; A(76):259-269.
24. Sarojini Krishnan K, Kanakam H, Charles C, Muthu S. Synthesis, structural, spectroscopic studies, NBO analysis, NLO and HOMO-LUMO of 4-methyl-N-(3-nitrophenyl)benzene sulfonamide with experimental and theoretical approaches, Spectrochimica Acta. 2013; A(108):159-170.